

Published in final edited form as:

Arterioscler Thromb Vasc Biol. 2009 April ; 29(4): 465–471. doi:10.1161/ATVBAHA.109.184234.

Dominant-negative loss of PPAR γ function enhances smooth muscle cell proliferation, migration, and vascular remodeling

Dane Meredith^{1,*}, Manikandan Panchatcharam^{2,*}, Sumitra Miriyala², Yau-Sheng Tsai³, Andrew J. Morris², Nobuyo Maeda³, George A. Stouffer¹, and Susan S. Smyth^{2,4}

¹Carolina Cardiovascular Biology Center, The University of North Carolina at Chapel Hill, Chapel Hill, NC 27599, Richard_Meredith@med.unc.edu, Rick_Stouffer@med.unc.edu

²Division of Cardiovascular Medicine, The Gill Heart Institute, University of Kentucky, Lexington, KY 40536, mpanc2@email.uky.edu, smiri2@email.uky.edu, a.j.morris@uky.edu

³Department of Pathology, The University of North Carolina at Chapel Hill, Chapel Hill, NC 27599, nobuyo@med.unc.edu, yausheng.tsai@pathology.unc.edu

⁴Department of Veterans Affairs Medical Center, Lexington, Kentucky 40511, susansmyth@uky.edu

Abstract

Objective—The Peroxisome Proliferator Activated Receptor-gamma (PPAR γ) protein is a nuclear transcriptional activator with importance in diabetes management as the molecular target for the thiazolidinedione (TZD) family of drugs. Substantial evidence indicates that the TZD family of PPAR γ agonists may retard the development of atherosclerosis. However, recent clinical data has suggested that at least one TZD may increase the risk of myocardial infarction and death from cardiovascular disease. In this study, we used a genetic approach to disrupt PPAR γ signaling to probe the protein's role in smooth muscle cell (SMC) responses that are important for atherosclerosis.

Results/Methods—SMC isolated from transgenic mice harboring the dominant-negative P465L mutation in PPAR γ (PPAR $\gamma^{L/+}$) exhibited greater proliferation and migration than did wild-type cells. Upregulation of ETS-1, but not ERK activation, correlated with enhanced proliferative and migratory responses PPAR $\gamma^{L/+}$ SMCs. Following arterial injury, PPAR $\gamma^{L/+}$ mice had a ~ 4.3-fold increase in the development of intimal hyperplasia.

Conclusion—These findings are consistent with a normal role for PPAR γ in inhibiting SMC migration and proliferation in the context of restenosis or atherosclerosis.

INTRODUCTION

PPAR γ , a dynamic nuclear transcriptional regulator, has well characterized roles in adipocyte differentiation¹, lipid metabolism² and insulin sensitivity^{3, 4}. Clinically PPAR γ is the molecular target of the insulin sensitizing thiazolidinedione (TZD) class of drugs that includes rosiglitazone and pioglitazone⁵. TZD⁶ and other PPAR γ agonists⁷ effectively increase insulin sensitivity in type 2 diabetic patients. Many preclinical and clinical studies have suggested that PPAR γ agonists protect against the development of atherosclerosis^{8–11} and reduce the development of intimal hyperplasia^{9, 12–14}. In the PROACTIVE trial, the PPAR γ agonist pioglitazone had beneficial effects on the combined secondary endpoints of myocardial

Address correspondence to: Susan S. Smyth, MD PhD, The Gill Heart Institute, 326 Charles T Wethington Building, 900 S. Limestone Street, Lexington, KY 40536, susansmyth@uky.edu.

*these authors contributed equally

infarction, stroke and death¹⁵. However a recent meta-analysis suggested that the use of the PPAR γ agonist rosiglitazone for the treatment of diabetes was associated with an increase in risk of myocardial infarction and a trend towards a higher risk of cardiovascular death¹⁶. Endogenous ligands for PPAR γ include unsaturated and oxidized fatty acids, eicosanoids, prostaglandins and possibly lysophospholipids. The putative PPAR γ agonist lysophosphatidic acid (LPA) accelerates neointimal formation after vessel injury in rodents in a PPAR γ -dependent manner¹⁷, suggesting that activation of PPAR γ may promote the development of intimal hyperplasia. However, at present, the role that PPAR γ plays in regulating vascular responses that underlie atherosclerosis and restenosis remain incompletely understood.

Proliferation and migration of vascular smooth muscle cells (SMCs) are key events in the development of intimal hyperplasia that occurs in the context of atherosclerosis and restenosis¹⁸. PPAR γ is present in vascular SMCs¹⁹, and the atheroprotective effects of PPAR γ ligands have been proposed to relate in part to beneficial effects on SMC biology. Indeed, studies have shown that TZDs inhibit vascular SMC proliferation^{12, 13} and migration^{12, 13, 20}, while increasing apoptosis²¹. It is not clear whether this is a direct effect of TZDs on PPAR γ or an “off-target” effect of the drugs, as most studies have inferred a role for PPAR γ in atherosclerosis on the basis of results with pharmacologic interventions. Homozygous deficiency of PPAR γ is embryonic lethal¹. Atherosclerosis and the development of intimal hyperplasia in a vascular SMC-specific PPAR γ knock-out mouse have not been reported. However, there is genetic evidence to support a role for PPAR γ in SMC biology. For example, a generalized PPAR γ knock-out model was created by breeding floxed PPAR γ mice to Mox2-Cre mice to inactivate PPAR γ in the embryo but not in trophoblasts²². The resulting mice have hypotension and impaired SMC contraction. PPAR γ variants with dominant negative function have been documented in families of humans with insulin resistance, type II diabetes and hypertension. Dominant negative loss-of-function PPAR γ mutations have also been introduced into mice to phenocopy abnormalities identified in humans. In humans, the substitution of a leucine for proline at amino acid 465 (P465L) is associated with severe insulin-resistance and significantly reduced PPAR γ activity²³. The homologous mutation in mice, P467L, causes hypertension, abnormal fat distribution but not insulin resistance²⁴, and cerebral vascular dysfunction²⁵. Thus, mice with the PPAR γ -P465L mutation (PPAR $\gamma^{L/+}$ mice) may be a useful model to examine the role of PPAR γ signaling in SMC function.

In the present study, we examined the response of primary cultures of SMCs obtained from aortas of mice harboring the PPAR $\gamma^{L/+}$ mutation or sibling controls. We report increases in proliferation and migration that translated into enhanced neointimal hyperplasia following vascular injury *in vivo*.

METHODS

Animals

The generation and genotyping of 129/SvEv mice containing the P465L mutation in PPAR γ (PPAR $\gamma^{L/+}$) mutation has been previously described^{24, 25}. To minimize background-specific effects, the PPAR $\gamma^{L/+}$ mice on the 129/SvEv background were crossed with female C57BL/6J mice from Jackson laboratories to generate F1 mice with the same complement of genes varying only in the presence (PPAR $\gamma^{L/+}$) or absence (PPAR $\gamma^{+/+}$) of the P465L mutation. Carotid ligation was performed in eight week old wild type PPAR $\gamma^{+/+}$ and PPAR $\gamma^{L/+}$ sibling matched mice and analyzed as previously described^{26, 27}. Carotid arteries were stained with combined Mason's Trichrome and elastin stain. Serial sections taken at 0.4 mm intervals from the ligation for histomorphometric analysis.

Vascular Smooth Muscle Cells

Aortas from sibling-paired mice aged 4 and 6 weeks old were digested in collagenase (175 U/ml; Worthington, NJ) and then adventitial tissue removed with by gentle tractions using forceps. The adventitia-free aorta was incubated overnight in a Dulbecco's Modified Eagle Medium (DMEM) containing 10% Fetal Bovine Serum (FBS), and then digested with elastase (concentration 0.25mg/ml, Sigma, MO) and collagenase (175 U/ml) in Hank's Balanced Salt Solution to generate isolated cells. Cells were cultured in DMEM containing 0.5 ng/ml EGF, 5 µg/ml insulin, 2 ng/ml bFGF, 10% FBS, 100 units/ml penicillin, and 100 µg/ml streptomycin. SMCs were isolated from endothelial cells by magnetic bead separation system (Invitrogen, Carlsbad, CA) and cell purity verified by SM α -actin staining.

For proliferation assays, cells at 70% confluence were serum starved in a 0.1% FBS for 72 hours and then plated at a concentration of 5,000 cells/well on a 96-well plate. Cells were treated with 0.1% BSA in PBS (vehicle), 20 ng/ml mouse platelet derived growth factor-BB (PDGF-BB, Ray Biotech, GA), or 10% FBS. The number of viable cells was quantified after 24, 48, 72, and 96 through incubation for 2 hours in a WST-1 solution (Biochain, CA). WST-1 is cleaved by mitochondrial succinate-tetrazolium reductase in viable cells to form formazan dye. The amount of formazan is proportional to the number of viable cells. After 2 hours of incubation in WST-1, absorbance at 450 nm was measured. For ERK activity, cells were washed with ice cold PBS and lysed (10 mM Tris-HCl pH 7.2, 1% Nonidet P-40, 158 mM NaCl, 1 mM EDTA, 50 mM NaF, 1 mM PMSF, 10 µg/ml aprotinin, 10 µg/ml leupeptin, 1 mM sodium orthovanadate, 10 mM sodium pyrophosphate). Total protein in clarified cell lysates (16,000g \times 10 min) was determined (BCA protein assay; Pierce, Rockford, IL) and equal amounts loaded onto 10% SDS-PAGE. Immunoblotting was performed with antibodies to actin (Santa Cruz Biotechnology, Santa Cruz, CA), ERK/phospho-ERK Thr202/Tyr204, and ETS-1 (Santa Cruz) and quantified using the Odyssey infrared imaging system (LI-COR, Lincoln, NE). Equal sample loading was confirmed by Coomassie blue staining.

In the scratch migration assays, cells were grown to confluence and then serum starved for 72 hours at which time a 400 µm scratch was placed through the confluent layer of cells using the end of a 200 µl pipette tip. After 12 hours, migration into the scratch was imaged through phase contrast microscopy with a Leica DM IRB inverted microscope. Cells in at least three fields were manually counted and the area occupied measured with NIH Image J software. In separate experiments, chemotactic migration was assessed by placing serum starved cells (1.8×10^4 cells/well) in the upper well of a chamber of a multiwellchambers (Neuroprobe Inc., Gaithersburg, MD) with a polyvinylpyrrolidone-free polycarbonate filter (5 µm pore). The bottom chamber was filled with DMEM containing 0.1% FBS and the indicated chemotactic agent (1 µM LPA [18:1 LPA in 0.1% BSA; Avanti Polar Lipids], 10% FBS, 20 ng/ml PDGF) or vehicle. The chamber was incubated for 12-h at 37°C in a CO₂ incubator, at which time the filter was removed from the chamber and the non-migrated cells were scraped from the upper surface. The membranes were fixed, and the migrated cells stained with Diff-Quik® (VWR Scientific Products, West Chester, PA). Digital images of the membranes were obtained with a Nikon 80i microscope using a 20 \times objective (NA = 0.5). The total area (µm²) occupied by migrated cells was determined with Metamorph imaging software.

For siRNA experiments, SMCs were placed in serum and antibiotic-free medium (10% (v/v) FBS in DMEM) at least 2 h before transfection and incubated with approximately 100nM of siRNA oligonucleotides to ETS-1 and scrambled control (Dharmacon, Lafayette, CO) and 1µl/cm² plate of X-tremeGENE siRNA Transfection Reagent (Roche, Indianapolis, IN). siGLO Green Transfection Indicator was used as a qualitative indicator of delivery. After 24 hours, the medium was changed to low or high glucose DMEM medium containing antibiotics (10% (v/v) FBS, 1% (m/v) penicillin and streptomycin and the chemotactic migration assay was performed as described above.

Statistical analysis

In vitro experiments were performed a minimum of three times with cells prepared from at least three different cohorts of animals. All results were expressed as mean \pm standard error of the mean (se). All data was analyzed using non-paired t-test or ANOVA, where indicated, using Sigma-STAT software, version 3.5 (Systat Software, Inc. San Jose, CA). A p-value of less than 0.05 was considered significant.

RESULTS

PPAR $\gamma^{L/+}$ vascular smooth muscle cells exhibit enhanced proliferation and migration

A key element in the development of neointima is the proliferation and migration of SMCs from the vessel media to intima. Studies using synthetic PPAR γ agonists such as TZDs have identified a potential role for PPAR γ as a regulator of SMC proliferation and migration. To probe the normal role of PPAR γ in SMC responses, we employed a genetic strategy in which PPAR γ activity was attenuated by the introduction of a dominant-negative PPAR γ mutation in mice. SMCs were isolated from aortas of wild-type mice or heterozygous knock-in mice carrying the dominant negative P465L mutation in PPAR γ (PPAR $\gamma^{L/+}$) and their proliferative properties examined. PPAR $\gamma^{L/+}$ SMCs displayed a modest 1.6-fold increase in proliferation in response to 10% FBS as compared to wild-type PPAR $\gamma^{+/+}$ cells at 72 hours ($P = 0.003$; Supplemental Figure 1). The enhanced proliferation was not observed in vehicle-treated PPAR $\gamma^{L/+}$ cells or in the presence of PDGF (Supplemental Figure 1).

PPAR $\gamma^{L/+}$ SMCs also displayed enhanced wound closure in a scratch assay (Figure 1A). Twelve hours after a single scratch injury, significantly more PPAR $\gamma^{L/+}$ SMCs migrated into the wound (108 ± 4 PPAR $\gamma^{L/+}$ cells versus 73 ± 3 wild-type PPAR $\gamma^{+/+}$ cells, $P = 0.002$, Figure 1B) and they migrated a greater distance (132 ± 7 μm for PPAR $\gamma^{L/+}$ cells compared 101 ± 7 μm for PPAR $\gamma^{+/+}$ cells; $P = 0.035$; Figure 2C). PDGF (20 ng/ml) increased the number of PPAR $\gamma^{+/+}$ cells and the distance they migrated and nearly rescued the defect in the PPAR $\gamma^{L/+}$ cells. In the presence of PDGF, 130 ± 4 PPAR $\gamma^{L/+}$ cells and 110 ± 2 PPAR $\gamma^{+/+}$ cells ($P = 0.011$) migrated a distance of 158 ± 3 μm and 153 ± 6 μm ($P = 0.49$), respectively (Figure 2C).

The behavior of wild-type PPAR $\gamma^{+/+}$ (Figure 2A) and mutant PPAR $\gamma^{L/+}$ (Figure 2B) cells was also measured in a chemotactic assay in which the cells migrated towards a gradient of FBS, PDGF, or lysophosphatidic acid (LPA), which, in addition to its well-described actions at cell surface receptors, has been proposed to also serve as a PPAR γ agonist²⁸. In wild-type PPAR $\gamma^{+/+}$ cells, migration increased 5.2 fold in the presence of FBS and 10-fold with LPA, whereas migration increased ~ 20 fold with the combination of FBS and LPA (Figure 2C). In comparison to wild-type cells, the migration of PPAR $\gamma^{L/+}$ cells was 6.1-fold higher towards FBS ($P = 0.002$, by ANOVA), 4-fold higher to PDGF ($P = 0.004$ by ANOVA), and 2.6-fold higher to LPA ($P = 0.002$ by ANOVA).

Mitogen-activated protein kinase pathways involving ERK contribute to SMC proliferative and migratory responses. We previously reported that SMC migration to FBS and LPA requires ERK activity²⁷. In keeping with these observations, the MEK1 inhibitor PD 98059 reduced chemotactic migration of wild-type PPAR $\gamma^{+/+}$ and PPAR $\gamma^{L/+}$ SMCs by 62% and 58%, respectively (Supplemental Figure 1). In addition, the TZDs rosiglitazone and pioglitazone inhibited wild-type PPAR $\gamma^{+/+}$ cell migration by $\sim 50\%$ and 40%. Interestingly, rosiglitazone but not pioglitazone partially blocked PPAR $\gamma^{L/+}$ cell migration by $\sim 40\%$ (Supplemental Figure 1).

TZDs have been variably proposed to alter ERK activity in SMCs, with some studies suggesting a role for TZDs in regulating cytosolic ERK²⁹ and other studies showing an effect downstream

of cytosolic ERK^{30, 31}. Therefore, we examined the effects of the PPAR γ P465L mutation on ERK activation in SMC. In wild-type PPAR $\gamma^{+/+}$ cells, FBS elicited an increase in ERK activity at 10 min that persisted for 60 min (Figure 3A). PDGF also increased ERK activity rapidly and resulted in a slight, but sustained elevation in ERK activity at 6 hours (Figure 4B). LPA stimulated a rapid increase in ERK phosphorylation that was maximal at 5 – 10 min (Figure 3C) and a second phase of late ERK activation. Biphasic ERK activation also occurs in thrombin stimulated SMC, where the second phase of ERK activation is triggered by HB-EGF expression³². No substantial differences were observed in ERK activation in mutant PPAR $\gamma^{L/+}$ cells in response to FBS (Figure 4A), PDGF (Figure 3B), or LPA (Figure 3C). Based on these results, the enhanced migration observed in the presence of the PPAR γ dominant negative mutation is unlikely to be the result of increased ERK activity. Others have reported that PPAR γ agonists prevent SMC migration by acting downstream of ERK to block expression of ETS-1³¹. ETS-1 also regulates the ability of PPAR γ agonists to inhibit telomerase activity in SMC³³. We therefore examined the effects of the dominant-negative PPAR γ P465L mutation on ETS-1. Following stimulation with FBS or PDGF, PPAR $\gamma^{L/+}$ cells upregulated ETS-1 to a significantly greater extent at earlier (~ 1 hour; P= 0.028) and later (~12 hours; P= 0.041) time points than did PPAR $\gamma^{+/+}$ cells (Figure 4A). Moreover, down regulation of ETS1 using RNA-dependent gene silencing (siRNA) blunted the enhanced PPAR $\gamma^{L/+}$ cell migration (Figure 4B).

PPAR $\gamma^{L/+}$ mice show increased neointimal formation during vascular remodeling

To determine if the enhanced SMC proliferation and migration observed in PPAR $\gamma^{L/+}$ SMC in culture also occurs *in vivo*, we examined the response to arterial injury in PPAR $\gamma^{+/+}$ and PPAR $\gamma^{L/+}$ mice using a well-characterized mouse model in which robust development of intimal hyperplasia occurs²⁶. At four weeks following carotid injury, intimal hyperplasia develops along the length of the vessel (Figure 5A and B). In response to injury, PPAR $\gamma^{L/+}$ mice develop more extensive neointima with a statistically greater intima/media ratio (Figure 5A and 5B; n = 8 PPAR $\gamma^{+/+}$, n = 9 PPAR $\gamma^{L/+}$). At 10 mm from the ligation, the PPAR $\gamma^{L/+}$ vessels display a 4.3 fold increase in neointima formation compared to the wild-type PPAR $\gamma^{L/+}$ vessel (P = 0.005 by ANOVA). The difference in intima:media ratio persisted until 24 mm from the ligation (Figure 5B). No difference in lumen (P = 0.317; Figure 5C) or medial (P = 0.447; Figure 5D) areas were observed between mice of different genotypes. Consistent with the observations in isolated cells, ETS-1 expression was higher in PPAR $\gamma^{L/+}$ vessels following injury (Figure 6).

DISCUSSION

Studies in animal models have shown that PPAR γ agonists inhibit atherosclerotic development¹⁰. However, the precise role for PPAR γ signaling in vascular SMCs remains unclear. In this report, we used a strain of mice harboring a dominant-negative acting PPAR γ allele that suppresses endogenous PPAR γ function²⁴ to probe the normal role of PPAR γ signaling in SMC phenotypic modulation that is important for atherosclerosis and restenosis. SMCs with the PPAR γ P465L mutation display dramatically enhanced migration and a modest increase in proliferation in *in vitro* assays. These *in vitro* observations appear relevant *in vivo* because mice with the PPAR γ P465L mutation exhibit exaggerated development of intimal hyperplasia following arterial injury. Upregulation of ETS-1 correlates with the enhanced migration in PPAR $\gamma^{L/+}$ SMCs, and transient reduction of ETS-1 inhibited PPAR $\gamma^{L/+}$ SMC migration. ETS-1 levels were also higher in PPAR $\gamma^{L/+}$ arteries after injury. Our findings are consistent with previous demonstrations that ETS-1 mediates the effects of PPAR γ agonists on migration³¹ and telomerase activity³³. Interestingly, although ERK activation contributes to SMC migration, we did not observe substantial differences in ERK activation in WT and

PPAR $\gamma^{L/+}$ SMCs. Others have also suggested that the anti-migratory effects of TZDs occur down-stream of ERK³¹.

Our results are consistent with a normal role for PPAR γ in attenuating injury-induced SMC proliferation, migration, and vascular remodeling. Our findings are in agreement with previous studies documenting inhibition of neointimal formation by TZD agonists in animal models³⁴ and a slowing of progression of carotid intima-media thickness by TZDs in individuals with Type2 diabetes³⁵. The beneficial effects of TZDs in nondiabetic preclinical models and our results in nondiabetic mice suggest that the reduction in intimal hyperplasia associated with PPAR γ activity is not simply a consequence of normalizing blood glucose and other metabolic abnormalities of diabetes. Because the PPAR γ P465L mutation may affect signaling through other PPAR isoforms⁹, we can not exclude a role of PPAR α or PPAR δ in regulating SMC responses. However our results, when considered in the context of the beneficial effects of TZDs, are most consistent with a central role of PPAR γ in attenuating SMC proliferative and migratory responses in the context of vascular injury. While our results suggest a direct role for PPAR signaling in SMCs, effects in other vascular cells, such as monocytes and endothelial cells, may also indirectly influence SMC function following arterial injury. Together with published experiments using pharmacologic approaches, our observations in a genetic model of altered PPAR γ activity support a role for endogenous PPAR γ in modulating important pathophysiologic processes underlying restenosis and atherosclerosis.

Surprisingly, rosiglitazone but not pioglitazone was able to suppress migration and proliferation in cells from mice with the PPAR γ P465L mutation. The lack of effect of pioglitazone was specific, in that under identical conditions, both pioglitazone and rosiglitazone inhibited wild-type SMC migration and proliferation. These findings would be consistent with rosiglitazone eliciting “off-target” effects that are not mediated by PPAR γ . In this context it is interesting to note that clinical trials have tended to show a beneficial vascular effect of pioglitazone¹⁵ but not of rosiglitazone¹⁶. It is possible, however, that the PPAR $\gamma^{L/+}$ cells have low levels of PPAR γ activity that for unknown reasons are selectively enhanced by rosiglitazone but not pioglitazone.

Our findings are also relevant to the role of the lysolipid mediator LPA in regulating SMC responses. In addition to acting on G-protein coupled receptors, LPA has been proposed as an endogenous agonist of PPAR γ ²⁸. In contrast to the inhibitory effects on the development of intimal hyperplasia reported with the TZD class of agonists, infusion of LPA into rodent carotid arteries has been associated with the formation of neointimal hyperplasia in a PPAR γ -dependent manner¹⁷. We observed enhanced LPA-migration in SMC with the dominant-negative loss-of-function PPAR $\gamma^{L/+}$ mutation, which appears to be non-selective with regards to agonists in that PPAR $\gamma^{L/+}$ SMC migration to PDGF was also enhanced. Our results suggest that LPA-, FBS- and PDGF-promoted chemotactic migration of SMCs is normally inhibited by PPAR γ -dependent pathways. Whether PPAR γ mediates other effects of LPA on vascular SMC function or regulates the effects of *endogenous* LPA is not known.

In conclusion, our findings are consistent with a normal role for PPAR γ in attenuating SMC migratory and proliferative properties which translate into beneficial vascular effects in terms of limiting the development of neointima. If future studies substantiate the initial reports of an association of at least one TZD with higher rates of adverse cardiovascular events, our results might suggest that the adverse cardiovascular profile for TZDs are due either to “off-target” effects or are the result of proatherothrombotic effects mediated by PPAR γ agonism in other blood and vascular cells.

Supplementary Material

Refer to Web version on PubMed Central for supplementary material.

Acknowledgments

The authors wish to thank Kirk McNaughton and Alyssa Moore for excellent technical assistance.

Disclosures This work was supported by NIH grants HL078663 and HL074219 to S.S.S. and DK67320 to NM. S.S.S. received Atorvastatin Research Award from Pfizer and previous grant funding from Takeda Pharmaceuticals.

Reference List

1. Barak Y, Nelson MC, Ong ES, Jones YZ, Ruiz-Lozano P, Chien KR, Koder A, Evans RM. PPAR gamma is required for placental, cardiac, and adipose tissue development. *Mol Cell* 1999;4:585–595. [PubMed: 10549290]
2. Schoonjans K, Peinado-Onsurbe J, Lefebvre AM, Heyman RA, Briggs M, Deeb S, Staels B, Auwerx J. PPARalpha and PPARgamma activators direct a distinct tissue-specific transcriptional response via a PPRE in the lipoprotein lipase gene. *EMBO J* 1996;15:5336–5348. [PubMed: 8895578]
3. Rangwala SM, Rhoades B, Shapiro JS, Rich AS, Kim JK, Shulman GI, Kaestner KH, Lazar MA. Genetic modulation of PPARgamma phosphorylation regulates insulin sensitivity. *Dev Cell* 2003;5:657–663. [PubMed: 14536066]
4. Hevener AL, He W, Barak Y, Le J, Bandyopadhyay G, Olson P, Wilkes J, Evans RM, Olefsky J. Muscle-specific Pparg deletion causes insulin resistance. *Nat Med* 2003;9:1491–1497. [PubMed: 14625542]
5. Lehmann JM, Moore LB, Smith-Oliver TA, Wilkison WO, Willson TM, Kliewer SA. An antidiabetic thiazolidinedione is a high affinity ligand for peroxisome proliferator-activated receptor gamma (PPAR gamma). *J Biol Chem* 1995;270:12953–12956. [PubMed: 7768881]
6. Nolan JJ, Ludvik B, Beerdsen P, Joyce M, Olefsky J. Improvement in glucose tolerance and insulin resistance in obese subjects treated with troglitazone. *N Engl J Med* 1994;331:1188–1193. [PubMed: 7935656]
7. Berger J, Leibowitz MD, Doebber TW, Elbrecht A, Zhang B, Zhou G, Biswas C, Cullinan CA, Hayes NS, Li Y, Tanen M, Ventre J, Wu MS, Berger GD, Mosley R, Marquis R, Santini C, Sahoo SP, Tolman RL, Smith RG, Moller DE. Novel peroxisome proliferator-activated receptor (PPAR) gamma and PPARdelta ligands produce distinct biological effects. *J Biol Chem* 1999;274:6718–6725. [PubMed: 10037770]
8. Chawla A, Boisvert WA, Lee CH, Laffitte BA, Barak Y, Joseph SB, Liao D, Nagy L, Edwards PA, Curtiss LK, Evans RM, Tontonoz P. A PPAR gamma-LXR-ABCA1 pathway in macrophages is involved in cholesterol efflux and atherogenesis. *Mol Cell* 2001;7:161–171. [PubMed: 11172721]
9. Duan SZ, Usher MG, Mortensen RM. Peroxisome proliferator-activated receptor-gamma-mediated effects in the vasculature. *Circ Res* 2008;102:283–294. [PubMed: 18276926]
10. Li AC, Brown KK, Silvestre MJ, Willson TM, Palinski W, Glass CK. Peroxisome proliferator-activated receptor gamma ligands inhibit development of atherosclerosis in LDL receptor-deficient mice. *J Clin Invest* 2000;106:523–531. [PubMed: 10953027]
11. Marfella R, D'Amico M, Esposito K, Baldi A, Di FC, Siniscalchi M, Sasso FC, Portoghese M, Cirillo F, Cacciapuoti F, Carbonara O, Crescenzi B, Baldi F, Ceriello A, Nicoletti GF, D'Andrea F, Verza M, Coppola L, Rossi F, Giugliano D. The ubiquitin-proteasome system and inflammatory activity in diabetic atherosclerotic plaques: effects of rosiglitazone treatment. *Diabetes* 2006;55:622–632. [PubMed: 16505224]
12. Law RE, Meehan WP, Xi XP, Graf K, Wuthrich DA, Coats W, Faxon D, Hsueh WA. Troglitazone inhibits vascular smooth muscle cell growth and intimal hyperplasia. *J Clin Invest* 1996;98:1897–1905. [PubMed: 8878442]
13. Law RE, Goetze S, Xi XP, Jackson S, Kawano Y, Demer L, Fishbein MC, Meehan WP, Hsueh WA. Expression and function of PPARgamma in rat and human vascular smooth muscle cells. *Circulation* 2000;101:1311–1318. [PubMed: 10725292]

14. Minamikawa J, Tanaka S, Yamauchi M, Inoue D, Koshiyama H. Potent inhibitory effect of troglitazone on carotid arterial wall thickness in type 2 diabetes. *J Clin Endocrinol Metab* 1998;83:1818–1820. [PubMed: 9589700]
15. Dormandy JA, Charbonnel B, Eckland DJ, Erdmann E, Massi-Benedetti M, Moules IK, Skene AM, Tan MH, Lefebvre PJ, Murray GD, Standl E, Wilcox RG, Wilhelmsen L, Betteridge J, Birkeland K, Golay A, Heine RJ, Koranyi L, Laakso M, Mokan M, Norkus A, Pirags V, Podar T, Scheen A, Scherbaum W, Schernthaner G, Schmitz O, Skrha J, Smith U, Taton J. Secondary prevention of macrovascular events in patients with type 2 diabetes in the PROactive Study (PROspective pioglitAzone Clinical Trial In macroVascular Events): a randomised controlled trial. *Lancet* 2005;366:1279–1289. [PubMed: 16214598]
16. Nissen SE, Wolski K. Effect of rosiglitazone on the risk of myocardial infarction and death from cardiovascular causes. *N Engl J Med* 2007;356:2457–2471. [PubMed: 17517853]
17. Zhang C, Baker DL, Yasuda S, Makarova N, Balazs L, Johnson LR, Marathe GK, McIntyre TM, Xu Y, Prestwich GD, Byun HS, Bittman R, Tigyi G. Lysophosphatidic acid induces neointima formation through PPARgamma activation. *J Exp Med* 2004;199:763–774. [PubMed: 15007093]
18. Ross R. The pathogenesis of atherosclerosis: a perspective for the 1990s. *Nature* 1993;362:801–809. [PubMed: 8479518]
19. Marx N, Schonbeck U, Lazar MA, Libby P, Plutzky J. Peroxisome proliferator-activated receptor gamma activators inhibit gene expression and migration in human vascular smooth muscle cells. *Circ Res* 1998;83:1097–1103. [PubMed: 9831704]
20. Bruemmer D, Yin F, Liu J, Berger JP, Kiyono T, Chen J, Fleck E, Van Herle AJ, Forman BM, Law RE. Peroxisome proliferator-activated receptor gamma inhibits expression of minichromosome maintenance proteins in vascular smooth muscle cells. *Mol Endocrinol* 2003;17:1005–1018. [PubMed: 12677008]
21. Bruemmer D, Yin F, Liu J, Berger JP, Sakai T, Blaschke F, Fleck E, Van Herle AJ, Forman BM, Law RE. Regulation of the growth arrest and DNA damage-inducible gene 45 (GADD45) by peroxisome proliferator-activated receptor gamma in vascular smooth muscle cells. *Circ Res* 2003;93:e38–e47. [PubMed: 12881480]
22. Duan SZ, Ivashchenko CY, Whitesall SE, D'Alecy LG, Duquaine DC, Brosius FC III, Gonzalez FJ, Vinson C, Pierre MA, Milstone DS, Mortensen RM. Hypotension, lipodystrophy, and insulin resistance in generalized PPARgamma-deficient mice rescued from embryonic lethality. *J Clin Invest* 2007;117:812–822. [PubMed: 17304352]
23. Barroso I, Gurnell M, Crowley VE, Agostini M, Schwabe JW, Soos MA, Maslen GL, Williams TD, Lewis H, Schafer AJ, Chatterjee VK, O'Rahilly S. Dominant negative mutations in human PPARgamma associated with severe insulin resistance, diabetes mellitus and hypertension. *Nature* 1999;402:880–888. [PubMed: 10622252]
24. Tsai YS, Kim HJ, Takahashi N, Kim HS, Hagaman JR, Kim JK, Maeda N. Hypertension and abnormal fat distribution but not insulin resistance in mice with P465L PPARgamma. *J Clin Invest* 2004;114:240–249. [PubMed: 15254591]
25. Beyer AM, Baumbach GL, Halabi CM, Modrick ML, Lynch CM, Gerhold TD, Ghoneim SM, de Lange WJ, Keen HL, Tsai YS, Maeda N, Sigmund CD, Faraci FM. Interference with PPARgamma signaling causes cerebral vascular dysfunction, hypertrophy, and remodeling. *Hypertension* 2008;51:867–871. [PubMed: 18285614]
26. Kumar A, Lindner V. Remodeling with neointima formation in the mouse carotid artery after cessation of blood flow. *Arterioscler Thromb Vasc Biol* 1997;17:2238–2244. [PubMed: 9351395]
27. Panchatcharam M, Miriyala S, Yang F, Rojas M, End C, Vallant C, Dong A, Lynch K, Chen J, Morris AJ, Smyth SS. Lysophosphatidic acid receptors 1 and 2 play roles in regulation of vascular injury responses, but not blood pressure. *Circ Res* 2008;103ePrint
28. McIntyre TM, Pontsler AV, Silva AR, St HA, Xu Y, Hinshaw JC, Zimmerman GA, Hama K, Aoki J, Arai H, Prestwich GD. Identification of an intracellular receptor for lysophosphatidic acid (LPA): LPA is a transcellular PPARgamma agonist. *Proc Natl Acad Sci U S A* 2003;100:131–136. [PubMed: 12502787]
29. Hattori Y, Akimoto K, Kasai K. The effects of thiazolidinediones on vascular smooth muscle cell activation by angiotensin II. *Biochem Biophys Res Commun* 2000;273:1144–1149. [PubMed: 10891386]

30. Game BA, Maldonado A, He L, Huang Y. Pioglitazone inhibits MMP-1 expression in vascular smooth muscle cells through a mitogen-activated protein kinase-independent mechanism. *Atherosclerosis* 2005;178:249–256. [PubMed: 15694931]
31. Goetze S, Kintscher U, Kim S, Meehan WP, Kaneshiro K, Collins AR, Fleck E, Hsueh WA, Law RE. Peroxisome proliferator-activated receptor-gamma ligands inhibit nuclear but not cytosolic extracellular signal-regulated kinase/mitogen-activated protein kinase-regulated steps in vascular smooth muscle cell migration. *J Cardiovasc Pharmacol* 2001;38:909–921. [PubMed: 11707695]
32. Sastre AP, Grossmann S, Reusch HP, Schaefer M. Requirement of an intermediate gene expression for biphasic ERK1/2 activation in thrombin-stimulated vascular smooth muscle cells. *J Biol Chem* 2008;283:25871–25978. [PubMed: 18650426]
33. Ogawa D, Nomiyama T, Nakamachi T, Heywood EB, Stone JF, Berger JP, Law RE, Bruemmer D. Activation of peroxisome proliferator-activated receptor gamma suppresses telomerase activity in vascular smooth muscle cells. *Circ Res* 2006;98:e50–e59. [PubMed: 16556873]
34. Bruemmer D, Law RE. Thiazolidinedione regulation of smooth muscle cell proliferation. *Am J Med* 2003;115(Suppl 8A):87S–92S. [PubMed: 14678872]
35. Mazzone T, Meyer PM, Feinstein SB, Davidson MH, Kondos GT, D'Agostino RB Sr, Perez A, Provost JC, Haffner SM. Effect of pioglitazone compared with glimepiride on carotid intima-media thickness in type 2 diabetes: a randomized trial. *JAMA* 2006;296:2572–2581. [PubMed: 17101640]

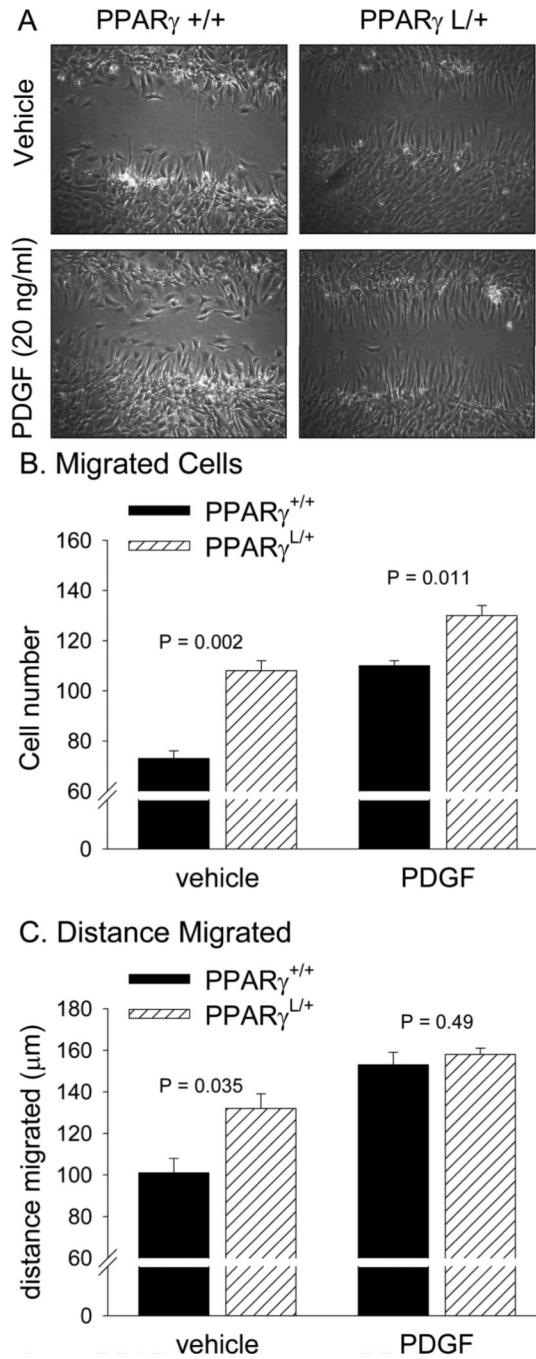


Figure 1. Enhanced wound closure in PPAR γ ^{L/+} aortic SMC

SMCs were grown to confluence, serum starved, and then a 400 μ m scratch was made through the lawn of confluent cells. After 12 hours, the region containing the scratch was imaged. The number of migrated cells was measured from digital images (A). Significantly more PPAR γ ^{L/+} SMCs migrated into the scratch (P = 0.002). The addition of PDGF to the media after scratch injury increased numbers of both PPAR γ ^{+/+} and PPAR γ ^{L/+} SMCs in the wound at 12 hours. (B); PPAR γ ^{L/+} cells migrated further into the wound than did PPAR γ ^{+/+} cells in the absence (P = 0.035) but not the presence of PDGF (P = 0.49). Values are presented as mean \pm se.

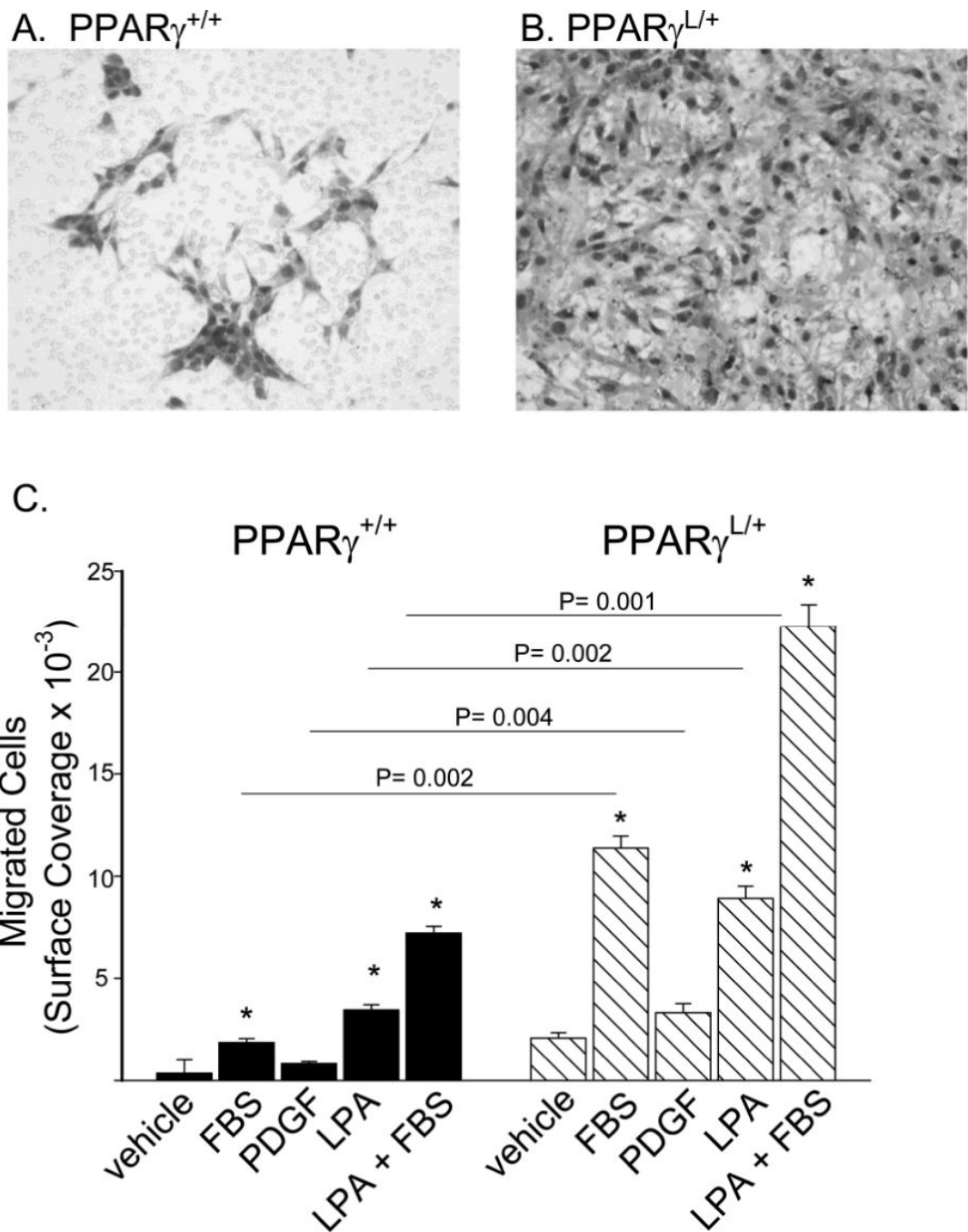


Figure 2. Enhanced migration in PPAR γ ^{L/+} SMC

SMCs were stained with Diff-Quik® on the undersurface of a membrane with a 5 μ m pore following migration to media containing vehicle, 10% FBS, 20 ng/ml PDGF, or 1 μ M LPA. Representative images of migrated PPAR γ ^{+/+} SMCs (A) and PPAR γ ^{L/+} SMCs (B). The area occupied by migrated cells is presented as mean \pm se (C). Combined results from three experiments are shown. *P<0.05 versus vehicle treatment by ANOVA. Values are presented as mean \pm se.

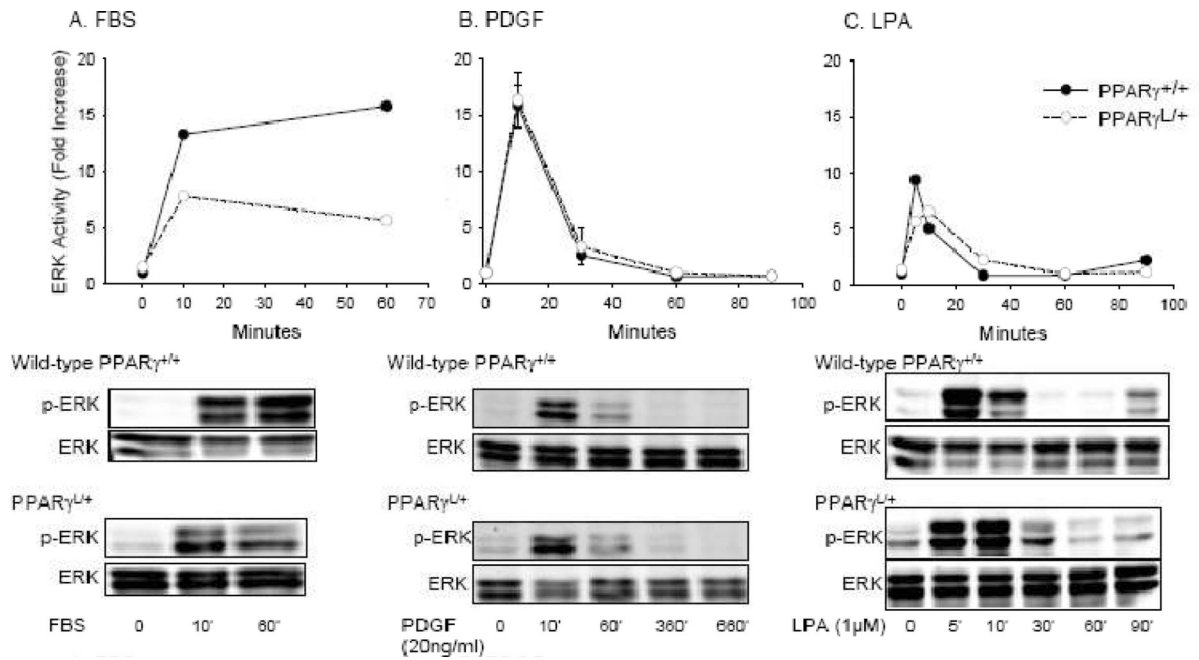
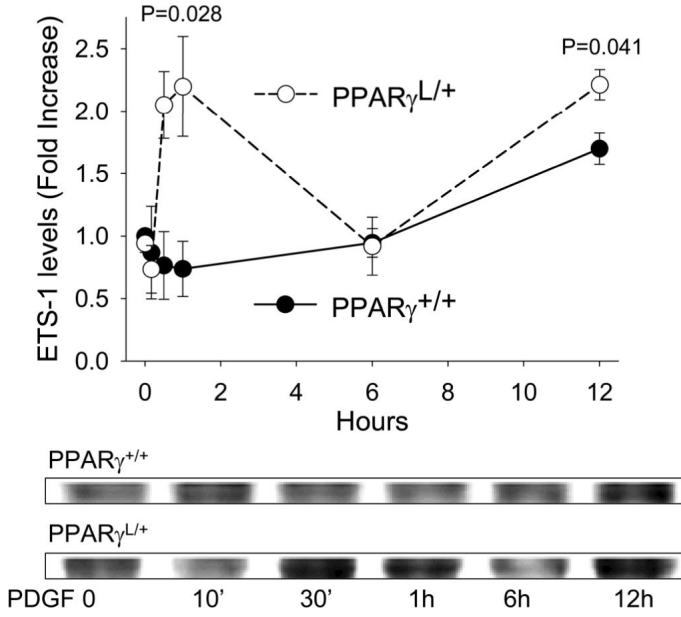


Figure 3. Normal ERK activation in PPAR $\gamma^{L/+}$ SMC

Time course of activation of ERK, as measured by phosphoERK/total ERK ratios, in cells following exposure to 10% FBS (A), 20 ng/ml PDGF (B), or 1 μ M LPA (C). Results are presented as mean \pm se and representative of three experiments with independent cultures of SMCs of each genotype.

A. ETS-1 Expression



B. PPAR $\gamma^{L/+}$ migration

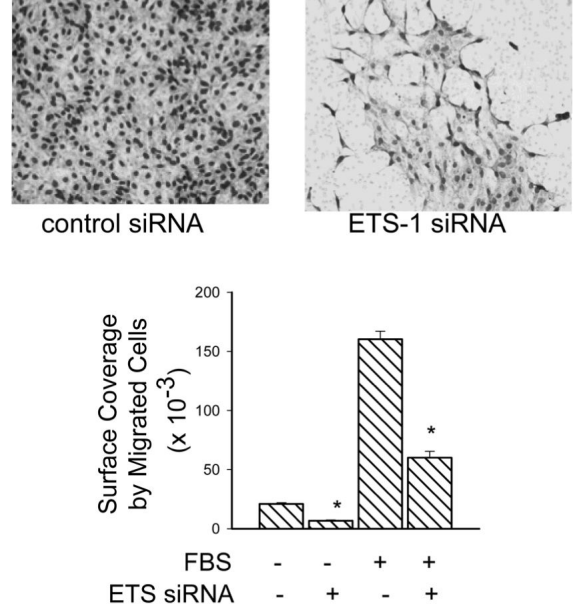


Figure 4. Alterations in ETS-1 in PPAR $\gamma^{L/+}$ SMC may account for enhanced migration
 (A) Time course of effects of 20 ng/ml PDGF on ETS-1 levels. Results are presented as mean \pm se and are representative of three experiments. (B) Migration of PPAR $\gamma^{L/+}$ was performed 72h after transfection with scrambled control siRNA or siRNA to ETS-1. Images are representative of results obtained in three experiments. Results are graphed as mean \pm sd. * P < 0.05.

NIH-PA Author Manuscript

NIH-PA Author Manuscript

NIH-PA Author Manuscript

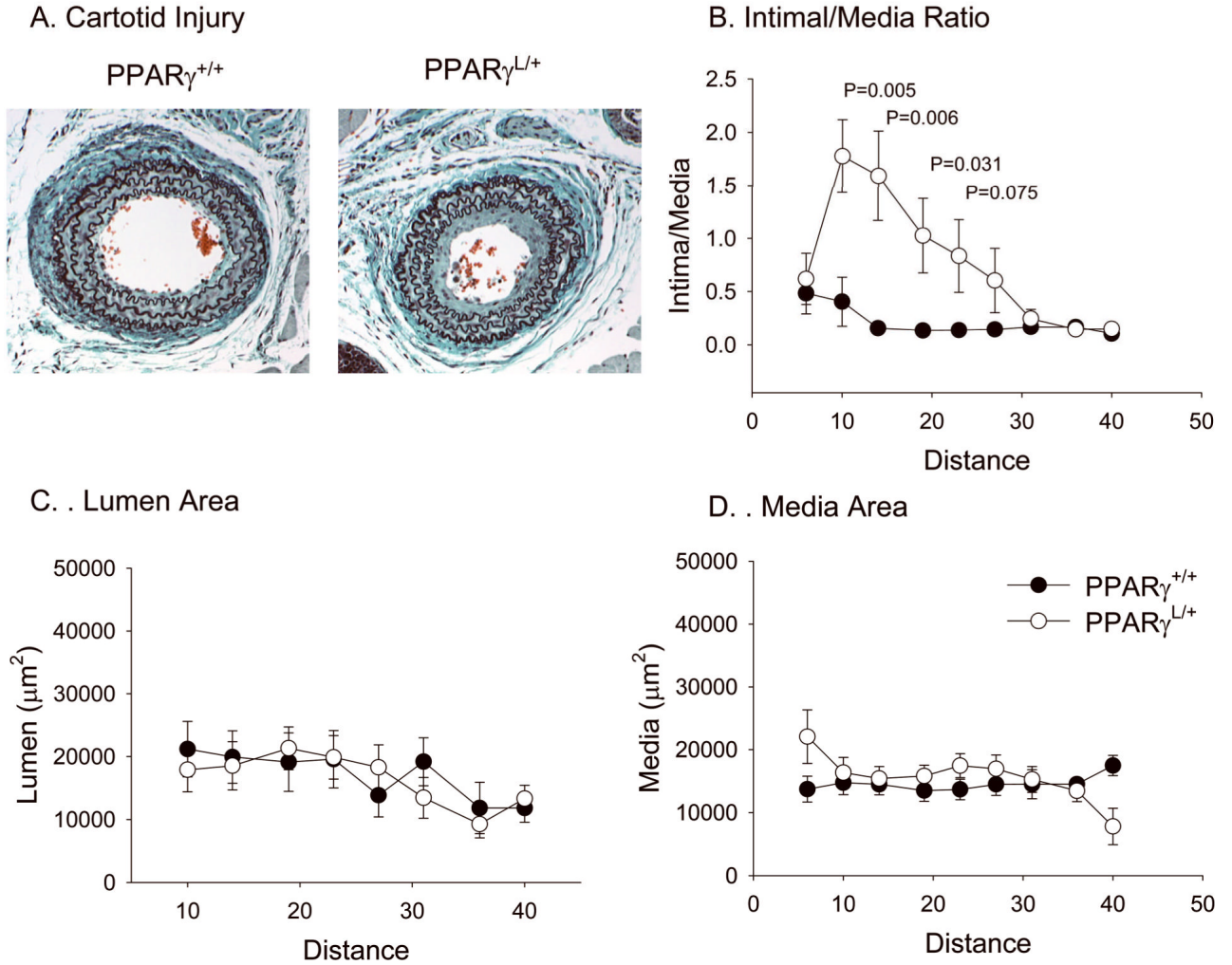


Figure 5. Enhanced remodeling in PPAR $\gamma^{L/+}$ mice in response to arterial injury
 Injured vessels were sectioned, imaged and measured with Image J to quantify vessel intima and media areas. Representative cross section of an injured PPAR $\gamma^{+/+}$ and PPAR $\gamma^{L/+}$ artery at 10 mm from the ligation (A). Intima to media ratios (B), lumen areas (C) and media areas (D) were calculated along the length of the vessel. Values are graphed as mean \pm se.

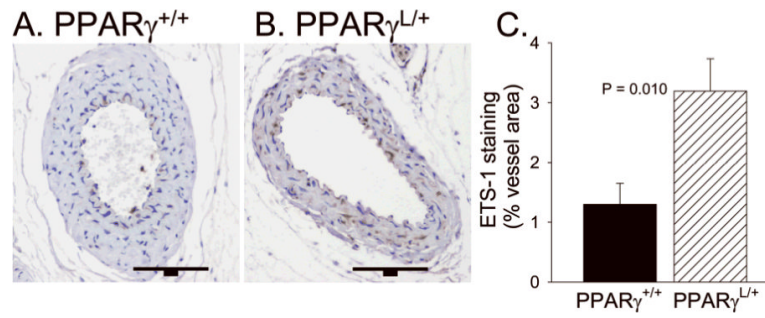


Figure 6. Upregulation of ETS-1 expression in PPAR $\gamma^{L/+}$ arteries after injury
 Immunohistochemistry for ETS-1 was performed on sections of injured vessels. Representative cross section of an injured PPAR $\gamma^{+/+}$ and PPAR $\gamma^{L/+}$ artery are presented. The bar is 100 μ m. The average area of ETS-1 in 5 vessels of each genotype is graphed (mean \pm se). *P < 0.05